29th Review of Atmospheric Transmission Models Meeting

13-14 June 2007
Museum of Our National Heritage
Lexington Massachusetts

Session 2: LIDAR

Invited Presentation ...

Chemical Species Measurements in the Atmosphere Using Lidar Techniques
Philbrick, C.R. (Slides & Paper)

White Light Lidar (WLL) Simulation and Measurements of Atmospheric Constituents
Brown, D.M., P.S. Edwards, Z. Liu and C.R. Philbrick (Slide Presentation)

Supercontinuum LIDAR Measurements of Atmospheric Constituents
Brown, D.M., P.S. Edwards, K. Shi, Z. Liu, and C.R. Philbrick (Paper)

Multistatic Lidar Measurements of Aerosol Multiple Scattering
Park, J.H., C.R. Philbrick and G. Roy (Slides & Paper)

CHEMICAL SPECIES MEASUREMENTS USING LIDAR TECHNIQUES

C. Russell Philbrick
Department of Electrical Engineering, Penn State University,
University Park, PA 16802

Abstract – **Laser remote sensing techniques provide opportunities for measuring primary natural atmospheric species and can be used to detect several of the hazardous or toxic species introduced into the atmosphere or deposited onto surfaces. In recent years, interest has increase in developing sensors capable of detecting lower concentration levels of various species for applications in air pollution monitoring, and for warnings of the presence of hazardous chemicals. Current capabilities are examined for various approaches using remote sensing techniques to measure concentrations of a wide range of chemical species. Our efforts and those reported by several other laboratories focus on development of various applications of Raman and DIAL lidar techniques to measure atmospheric species. New optical devices and improved electronics are leading to advances in these lidar instruments and expanding our measurement capabilities. The recent advent of femtosecond lasers and their use with photonic crystal fibers to generate supercontinuum, or white-light, sources have opened new opportunities for monitoring chemical species. These laser sources open the possibility of applying the well-developed techniques of hyper-spectral remote sensing to new ways of measuring path concentrations of molecular species, while using a controlled radiation source instead of sunlight or incoherent light sources. Advances in the traditional techniques and several new opportunities for remote detection of various molecular species using resonance processes (resonance Raman and fluorescence) are also explored. Recent results, simulations and calculations are used to describe current capabilities, and indicate future directions for laser remote sensing.**

I. INTRODUCTION

The goal of this paper is to summarize current capabilities and approaches being used and under development for detection of low concentrations of chemical species using optical absorption and scattering processes. The detection of chemical species depends upon several factors: sufficient signal strength, distinctive features in the detected signal, and uniqueness of the signal features of the chemical species of interest relative to the background interfering signals.

II. PROCESSES FOR SPECIES MEASUREMENTS

Each molecule making up a chemical sample is composed of a unique combination of elements that are held together with several types of bonds with differing bond strengths, and these factors lead to the unique set of quantized vibrational energy levels, which can be used to uniquely identify a chemical species. We can observe the uniqueness of each chemical species by observing the infrared absorption spectra in the 0-4200 cm^{-1} region, corresponding to wavelengths from about 40 to 2.4 μm. This spectral region contains many features corresponding to the energies for the vibrational, rotational, bending, stretching, and other oscillatory modes of the molecules in the optical spectrum; the most energetic being the vibration of the H_2 molecule at 4150 cm^{-1}. The spectra of molecules with hydrogen bonded to carbon, nitrogen, and oxygen are often observed in the region between 2.5 and 3.5 μm. There are higher energy spectral features (<2.5 μm); however these represent harmonic overtones, and the more energetic electronic activity of molecular and atomic bonds. In most cases, spectral features are well identified with the quantized energy states of oscillatory motions of molecules. In some of the more complicated long chain molecules, these features are identified with the sub-group clusters of molecules that attached in chain-like fashion. In even more complicated molecules or cell structures, only a few of the primary spectral features of cluster molecules and bond types may be distinctly identifiable in the absorption spectra.

The second major way of identifying a chemical species is by examining the scattered optical radiation, or Raman scattering spectrum. Molecular bonds, with any small asymmetry in the charge distribution of bound or shared electrons, can be forced into oscillation by the presence of an oscillatory electric field. Thus, any passing photon has the opportunity to be absorbed or scattered by a molecule and force the oscillation of the many different energetic modes in the chemical, if it is optically active or Raman active. The scattered photon can leave with less energy by a precise amount (red-shifted), which corresponds to the energy gained by the molecule; this is referred to Stokes component of the Raman spectrum. If the molecule already is residing in a higher energy oscillatory state, then the scattered photon may acquire additional energy, and the spectrum of the scattered radiation is referred to as anti-Stokes.

Additional optical techniques for chemical species analysis include Laser Inducted Breakdown Spectra (LIBS) and fluorescent emission. The LIBS technique uses a focused laser beam to rupture the molecular structure with intense electric fields, and in the process creates a large number of excited atomic states, which emit spectral components that can be often used to identify the likely parent species. Fluorescent emissions are excited in many molecules and these can be sometimes used to detect the presence of particular chemical

compounds. However, the fluorescence is more often useful to separate a class of materials, rather than to identify a particular species, because the combination of rapid radiationless transitions remove much of the specificity of which energy states were involved, and finally these often result in broadband emission. These last two techniques will not be elaborated on further in this report.

Infrared optical absorption and Raman scattering provide complementary pictures of the oscillatory resonances that exist within a molecule. Often the same energy state will appear as both infrared active and Raman active; while other energy states will only be observed in either the infrared absorption or in the Raman scatter spectra of a molecule. Both IR absorption spectra and Raman scatter intensity spectra provide "fingerprints" that are most specific in identifying molecules.

When the molecule is part of a lattice structure, in a liquid form, or smeared into a compound with other materials, the response of the energy states to the impinging radiation is altered in intensity, and may be shifted by the stiffening of the bonds between the atoms composing the molecular structure. However, the spectral features are often recognized to identify which chemical species are present.

A. Infrared Absorption

Molecular vibration is **infrared active** if the molecule's normal dipole moment is modulated. The impinging radiation field must be near the same frequency as an oscillation resonance for the electric dipole moment if the radiation is to be absorbed. The resonance occurs at an energy corresponding to a vibrational, rotational, stretching, bending, rocking, wagging, twisting, or other oscillatory energy states of a molecule. The infrared spectrum can be considered to extend from 1000 μm (10 cm^{-1}) to 0.7 μm (14,000 cm^{-1}); the sub-ranges are often referred to as near-IR (beginning 0.7 μm, 14,000 cm^{-1}), mid-IR (beginning 2.4 μm, 4,200 cm^{-1}), long-IR (beginning 8 μm, 1250 cm^{-1}), and far-IR (beginning 25 μm, 400 cm^{-1}). Most of the absorption features that are used for optical spectra identification are found in the region between 2.5 and 25 μm (4,000 to 400 cm^{-1}).

The spectrum of the absorption of optical radiation by the molecules of the background atmosphere is shown in Fig. 1. Here the atmospheric column absorption from space to the Earth's surface is shown using the MODTRAN™ atmospheric model [1]. The visible region between 0.4 and 0.7 μm is relatively free of absorption and scattering along the vertical path through the atmosphere, except for scattering by molecules (principally nitrogen and oxygen) and by aerosols. The ultraviolet region, between 0.2 μm and 0.4 μm, exhibits rapidly decreasing transmission at shorter wavelengths due to strongly increasing molecular scattering (~ $1/\lambda^4$) that gives way to even stronger UV absorption by ozone. Then below 0.2 μm, radiation is absorbed that dissociates the O_2 molecule, and at even shorter wavelengths, the radiation dissociates and ionizes all of the molecular species with essentially complete absorption of any radiation along the path. The infrared region between 0.7 and 2.5 μm contains the harmonic overtones of the strongly absorbing species. The region from 2.5 to 25 μm is the primary region of spectral signatures that are used to identify and quantify chemical species using optical absorption techniques.

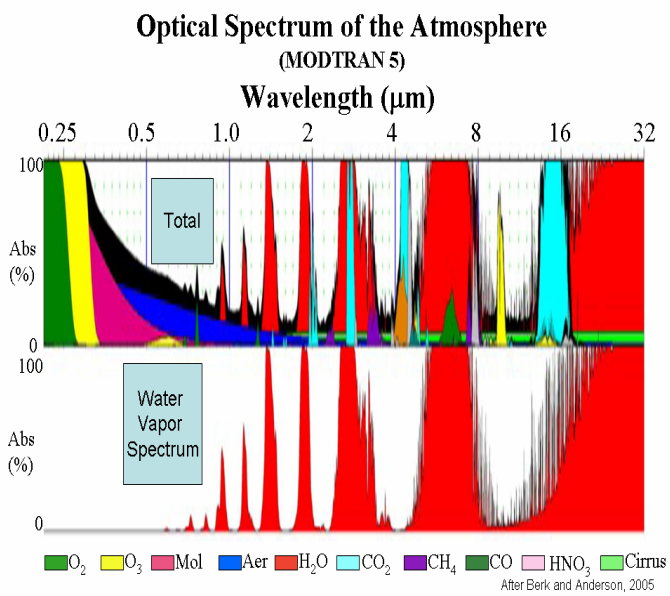

Figure 1. The vertical path integrated optical absorption between space and ground as calculated using the MODRAN model for optical propagation [1].

B. Raman Scatter

A molecule is **Raman active** if a dipole is induced by the action of the electric field of a scattering photon, which forces a relative motion between the electrons and the nuclei. The induced dipole moment is proportional to the radiation intensity's electric field strength and the polarizability of the molecule. Many of the same vibrational and other oscillatory energy states, which are responsible for the infrared absorption, when the molecule has an electric dipole moment, are also observed as shifts of scattered Raman signal intensities when a dipole moment is induced. In the case of Raman scattering, instead of signals located in the 2.5 to 25 μm wavelength region, the scattered signals are located at the energy difference of the oscillatory energy level from the excitation wavelength. The vibrational energy states are most useful for identifying and quantifying the species because of red shifting the incident energy by the magnitude of the vibrational resonances of the species of interest. The possibility of using the Raman scattering for lidar measurements was described in some detail in papers by Inaba and his colleagues since the 1970's [2-4]. The vibrational energy shifts are shown in Fig. 2 for several common species of interest [2]. The Nd:YAG laser has become the primary transmitter used for Raman lidar investigations during the past two decades. It has the advantage of providing a high output power, and the 1.064 μm fundamental wavelength can be used to generate 2nd, 3rd, and 4th harmonic outputs in the visible and ultraviolet wavelengths. In Fig. 2 the wavelengths of Raman scattered signals from N_2, O_2, and H_2O molecules are indicated for these laser lines.

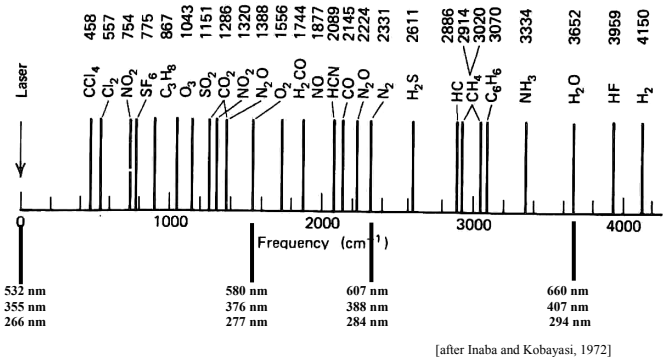

[after Inaba and Kobayasi, 1972]

Figure 2. The frequency shifts of several common molecules are indicated. These represent the energy difference for Stokes and anti-Stokes shifts toward the red and blue directions from the excitation source. The wavelengths expected for excitation by an Nd:YAG laser second, third and fourth harmonics are indicated for the N_2, O_2, and H_2O molecules [2].

C. Scattering Processes

The scattering of optical radiation by molecular species provides several different signals for detecting the presence of various chemical species and measuring their concentration and distribution. In Fig. 3, energy level diagrams are used to represent the several scattering processes that can be used to investigate chemical species.

Fig. 3 shows the several processes that occur as optical wavelengths interact with molecules. First, the infrared absorption process is depicted as absorbed energy raises a molecule to a higher vibrational level. The energies typically correspond to wavelengths between 2.5 and 25 μm. Many other types of oscillatory motions, which correspond to quantized energies of rotation, bending, etc., also can be observed as absorption features. The processes of scattering result in Rayleigh scatter, Mie scatter, and Raman scatter signals. In each of these cases, the interaction may be viewed as the molecule existing in a 'virtual energy' state (or condition) as the photon energy packet interacts with the molecule or aerosol particle. In most of the cases, the particle will return to the ground state and give back the same energy photon as was incident – except shifted slightly by the Doppler velocity of the scattering particle. The cross-section differences for the several interactions are indicated in Table I. The cross-section increases for molecules as the probe wavelength reduces toward smaller values (higher energy) as $1/\lambda^4$, and it increases when the aerosol increases in size as a^6.

TABLE I. APPROXIMATE CROSS-SECTIONS

Process	Type	Cross section (cm2/sr)	Use
Scattering	**Rayleigh**	**$\sim 10^{-26}$**	**Atmosphere T, r**
	Mie	**10^{-26}-10^{-8}**	**Aerosols, particles a, n, r**
	Raman		
	Non-resonance	**10^{-30}-10^{-28}**	**Molecules T, [Ni], a**
	Resonance	**10^{-28}-10^{-20}**	**[N_i]**
Absorption	**DIAL**	**10^{-24}-10^{-20}**	**[N_i]**
	DAS	**~(DIAL) x 10^4**	**N_i (path integrated)**
Emission	**Fluorescence**	**10^{-26}-10^{-20}**	**Species detection ~N_i (quenching)**

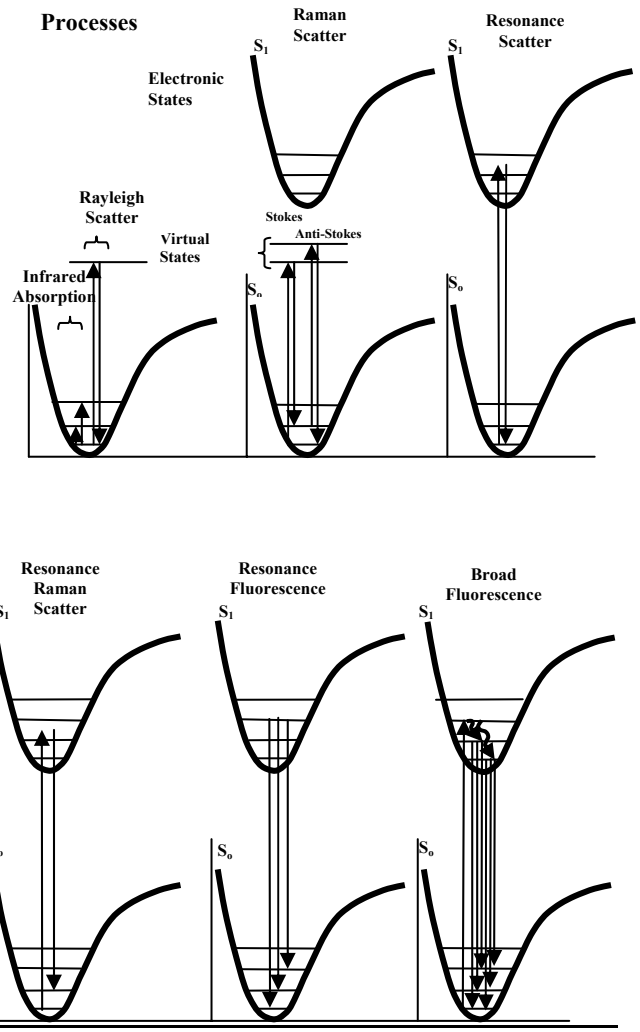

Figure 3. The several processes involving the interactions of incident optical radiation on molecules; processes include infrared absorption, Rayleigh scattering, Raman scattering, and resonance scattering processes.

As the molecule relaxes from the 'virtual energy condition,' it may return to a higher (Stokes) or a lower (anti-Stokes) energy state than its original one (if the molecule is Raman active – i.e. experiences an induced dipole moment), and thus the scattered photon will be red-shifted or blue-shifted from the initially incident one. Because the allowed final energy states correspond to the precise and discrete changes associated with the vibrational energy levels, it is then possible to identify the species and measure their concentrations using Raman scatter signals. Cross sections for Raman scatter at the Stokes (red-shifted) wavelengths are typically 10^3 smaller than the Rayleigh scatter at the central Cabannas line. In some cases, significant increases in the Raman cross-sections, see Table I, can be gained when the photon energy is near an electronic state. The added resonant response of the electronic state from the photon's electric field results in higher Raman scatter efficiency. When the photon energy is sufficient to directly excite the electronic states, then fluorescence emission is often observed.

D. Raman Lidar Measurements

The Raman scatter signals can be effectively used in lidar applications to measure species concentrations. Fig. 4 shows an example of water vapor measurements using the ratio of water vapor to nitrogen Raman signals [5-7].

The measurements of many atmospheric species can be obtained from the Raman scattered signal of the selected species in a ratio to the nitrogen signal. Since laboratory measurements have provided the accurate Raman cross-sections for most chemical species, the ratio to nitrogen provides accurate and robust profiles of the selected species concentration. By taking the ratio to the known nitrogen density, the density profile of the selected species is also known, and most of the instrument calibration values and system performance unknowns cancel out during the calculation of the species density. Another example of a minor species that we can measure using Raman scatter is shown in Fig. 5. The ozone profile is measured by using the ratio of the O_2 to N_2 signals from the 266 nm 4th harmonic of the Nd:YAG laser [7, 8].

The oxygen to nitrogen ratio should be constant in time, and through out the lower atmosphere, to within about 1:10^5. The two Raman scatter wavelengths, 277.6 nm (O_2) and 283.3 nm (N_2), occur on the steep slope of the Hartley absorption band of ozone, and thus any change in their relative signal ratio as a function of altitude must due to absorption. A survey shows that ozone is the species with a differential absorption for these two wavelengths. Since the accurate laboratory cross-sections for ozone are known the technique provides a very accurate and robust measurement of ozone. The only significant error is the signal/noise relationship, thus the measurements can be improved with higher power lasers or larger receiving telescopes. The lidar profile of ozone is compared in Fig. 5 with a simultaneously measured aircraft profile [9]. The large scatter differences in the data above 2 km are due to the limited lidar signals from longer ranges. The technique has been used for several intensive investigations of air quality [10-13].

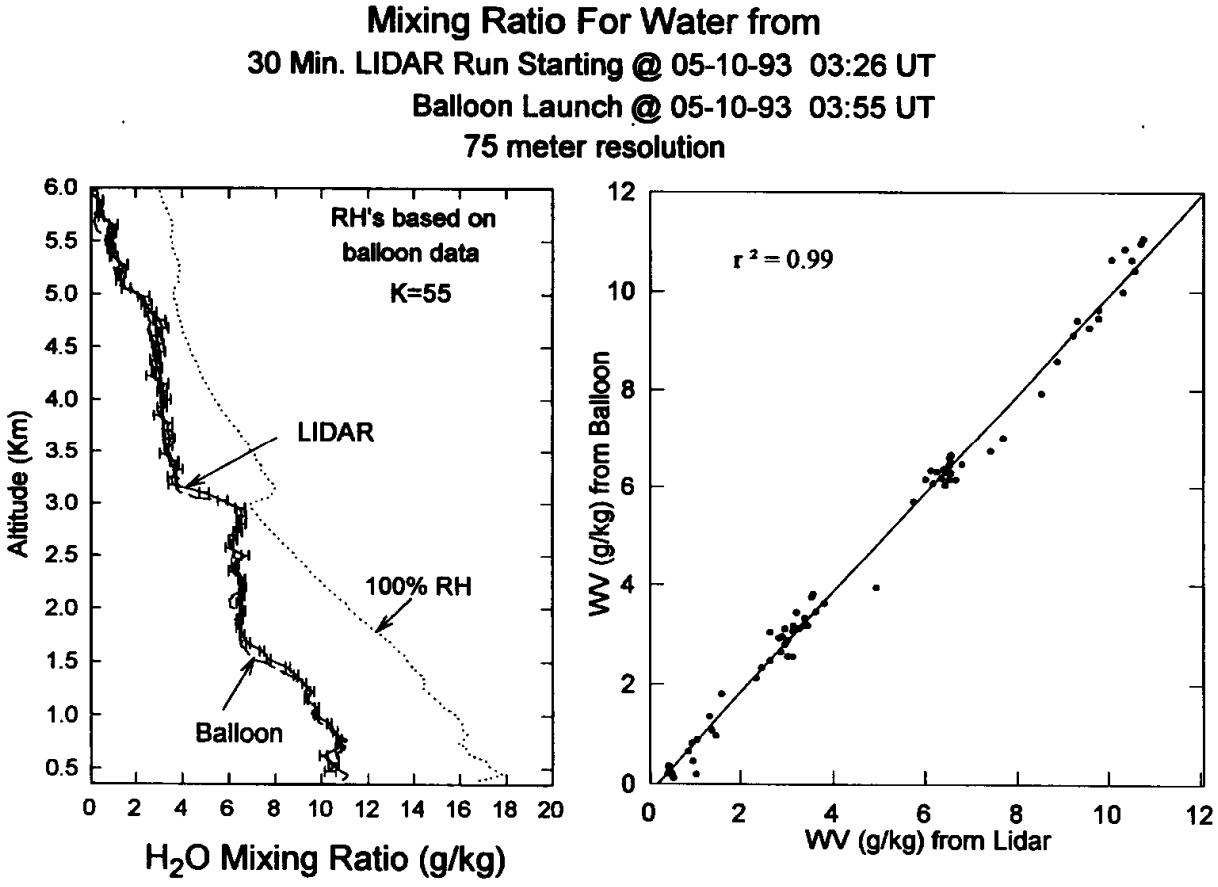

Figure 4. The water vapor specific humidity profiles measured with the PSU LAMP lidar system are compared with simultaneous Rawinsonde balloon release from Pt. Mugu, CA [6].

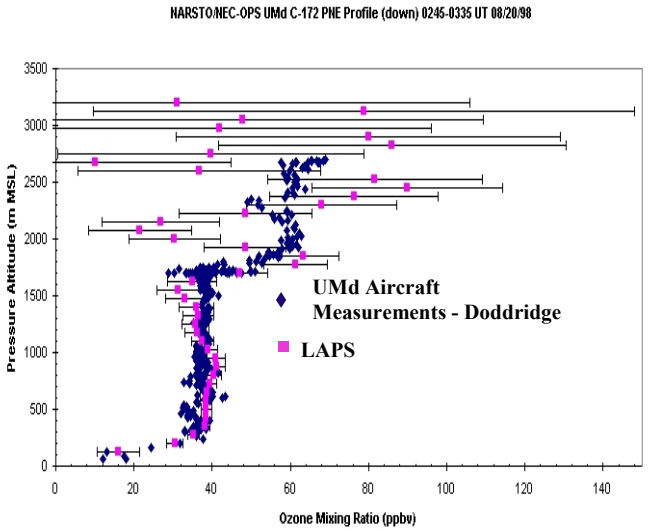

Figure 5. Raman lidar measurements of ozone are compared with simultaneous aircraft data [9].

The Raman lidar measurements of water vapor, and temperature from the rotational Raman scattered signals allows us to calculate the relative humidity and the RF refractivity. The relative humidity values are straight forward to calculate from Raman lidar measurements and are important for detecting the regions where sub-visual clouds begin to form [10-13]. The RF refractivity measurements are important for radar interpretation because of the ducting effecting on beam propagation [13-15]. Table II shows the analysis of the meteorological influences upon the RF refraction, and it demonstrates that it is the water vapor gradients that cause the largest effect on radar interpretation. Calculations of the attenuation of a radar beam in Fig. 6 show bending of the radar beam with the signal ducts bent over the horizon [14].

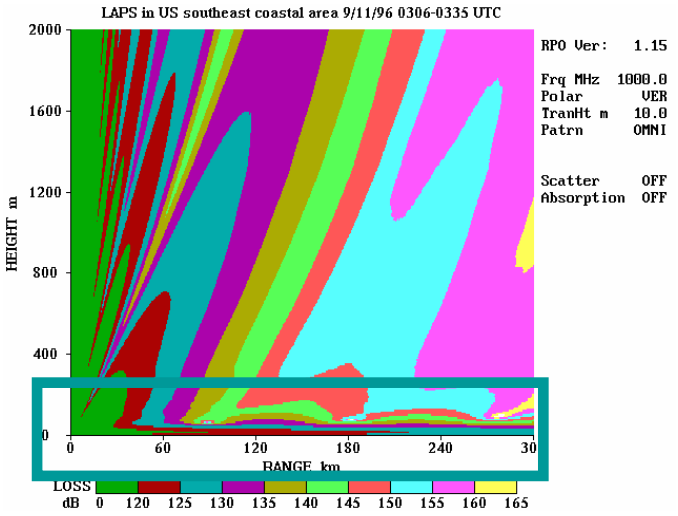

Figure 6. The equations above are used to calculate RF refraction and examine the water vapor influence, and the RPO (Refractive Propagation Optical) model is used with lidar data to show RF ducting effects during shipboard tests [13-15].

Table II. Calculation and sensitivity of RF-refraction

$$N = (n - 1) \times 10^6 = 77.6\, P/T + 3.73 \times 10^5\, e/T^2$$

$$e\ (mb) = (r\, P)/(r + 621.97)$$

P - surface pressure r - specific humidity T - temperature

$T(K) \sim 295$ K $P(mb) \sim 1000$ mb $r \sim 7$ g/kg $N \sim 310$

$N/r \sim 6.7$ $N/T \sim -1.35$ $N/P \sim 0.35$

$$dN/dz = 6.7\, dr/dz - 1.35\, dT/dz + 0.35\, dP/dz$$

Gradients in water vapor are most important in determining RF ducting conditions.

E. Differential Absorption Lidar (DIAL)

During the past four years, an effort by ITT Space Systems, supported by Penn State researchers, has resulted in development of a three wavelength mid-IR DIAL system that is capable of measuring natural gas pipeline leaks as an aircraft flies over the surveyed pipeline location [16-18]. The lidar is deployed in an aircraft so that long segments of pipeline can be rapidly surveyed. Fig. 7 shows an example of a pipeline leak detection superimposed onto visual imagery.

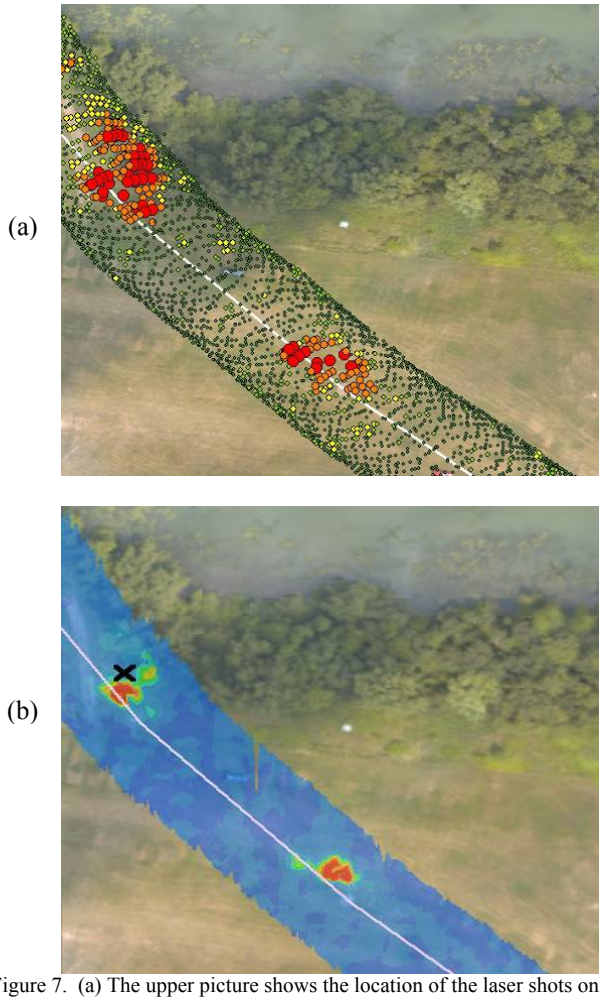

Figure 7. (a) The upper picture shows the location of the laser shots on the surface as the plane flies its course; (b) the locations of high methane concentrations that show leaks in the buried pipeline.

In the example shown in Fig. 7, the upper picture depicts the geospatial position of the laser spot locations on the ground image, with the threshold detection triggers indicated for individual shots. The lower picture shows the regions of high concentrations of methane leaking from a buried pipeline. This sensor has greatly advanced the capability for remote detection of trace concentrations of gases. The ANGEL system can survey hundreds of miles of pipeline in one day compared to earlier practice of sending a man in a jeep to survey 20 miles in a day. The instrument detects a leak with a single set of three near simultaneous laser shots, and the repetition rate is near 1 kHz as the aircraft follows a GPS determined pipeline route. Developing this system was a major undertaking, however it now appears on the way to becoming the first commercial DIAL lidar system.

F. Supercontinuum Laser for SPR-DIAL

The broad spectrum that can be achieved using a femtosecond laser pulse into a photonic crystal fiber opens a new opportunity for measurement and analysis of many wavelengths as DIAL pairs at the same time [19-21]. An example of the type of analysis that can be accomplished is indicated in Fig. 8. This figure shows the spectral features of water measured using the supercontinuum laser as transmitter for lidar, and is compared with the MODTRAN model calculated at the resolution of the spectrometer used in these experiments. Spectral Pattern Recognition – Differential Absorption Lidar (SPR-DIAL) provides many simultaneous wavelengths that can be used to advantage in some cases. The technique of using an extensive set of spectral features for a DIAL type analysis, as opposed to just using a paired on-line to off-line ratio to find the concentration has a major advantage in reducing measurement errors. The technique is being used to study atmospheric paths over distances of hundreds of meters at this time, and we expect that paths of kilometer lengths will be measured in the near future. The systems that have been used during the past two years have operated in the region from the ultraviolet (~350 nm) through the near-IR (~1.7 μm), but the next generation sensor will extend the measurements into the mid-IR (1.5-5 μm).

G. Resonance Raman and Fluorescence

In collaboration with colleagues from N.C. State University (research group of Hans Hallen), a PSU doctoral candidate, Adam Willitsford is investigating the properties of resonance Raman scattering. The topic is being pursued in an attempt to develop a new technique for detection of trace amounts of chemical smears on surface, particularly for applications to the stand-off detection of explosive materials. Our expectation is that the Raman spectra of interesting materials will have resonance responses as the incident probe wavelength approaches an electronic excitation at ultraviolet wavelengths. The deep ultraviolet wavelength region is also interesting for another reason. Since most fluorescent emissions occur at wavelengths longer than 280 nm, the fluorescent signature will not contaminate the Stokes components of the Raman spectra when the excitation laser wavelength is less than about 260 nm (the width of the full Raman spectrum is less than 25 nm). In addition to the sensitivity gain from molecular scatter cross-section as one selects shorter wavelengths, the resonance Raman process could increase the sensitivity by several orders of magnitude. As an example of an ultraviolet resonance Raman measurement, Fig. 9 shows the Raman spectrum of an ice surface for a sequence of measurements. In this case, the wavelength of the excitation laser is decreased in 2 nm steps from 275 to 245 nm. The sudden change in the Raman spectrum intensity between 3100 and 3600 cm^{-1} is apparent as the wavelength of the excitation source decreases from 271 to 269 nm. A wide range of materials are currently under investigation for their resonance Raman characteristics. Models of performance for this process are needed to take understand and take advantage of the opportunities offered by deep ultraviolet excitation.

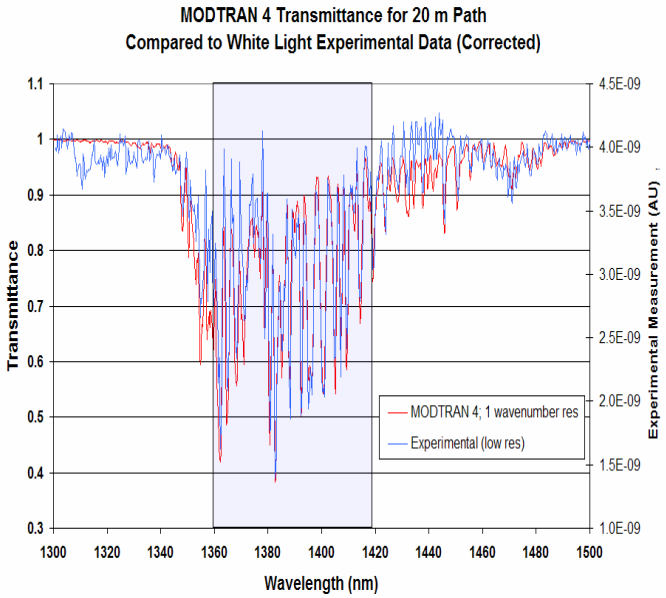

Figure 8. The water vapor spectrum measured using the PSU supercontinuum laser as a lidar transmitter with comparison to the MODTRAN model.

III. SUMMARY

Improved means for detection of chemical species and measurement of their concentrations in the atmosphere and on surfaces are a primary focus for several applications. Many needs exist in meeting requirements for detection of explosives and toxic chemicals for DoD and DHS, as well as for air pollution monitoring for state and federal agencies.

Table III lists the several techniques for optical sensors that would be most useful for detection and for measuring the concentration of chemical species; together with estimates of performance that could be expected with reasonable systems. Many factors influence the performance of such sensors, in particular, the transmitted intensity, receiver collection area, detector sensitivity, as well as the instrument operating environment and range to target.

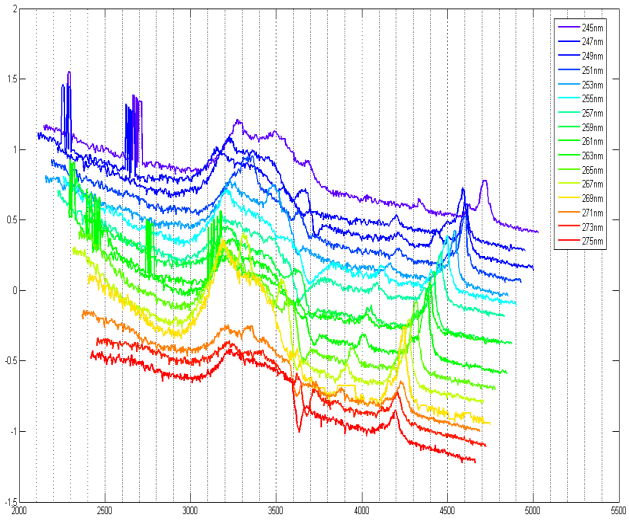

Figure 9. An offset sequence of Raman spectra obtained by scattering laser wavelengths from 275 to 245 nm on an ice surface (from private communication, Adam Willitsford).

TABLE III
PRIMARY METHODS FOR STANDOFF OPTICAL DETECTION ARE LISTED WITH ESTIMATES OF SENSOR PERFORMANCE

Optical Techniques and Detection Range (Est.)
DIAL ~ ppm
100 ppm – 10 ppb
DAS ~ 10's of ppb
10 ppm – 100 ppt
Raman ~ 100's ppm
1000 ppm – 10 ppm
Raman/DIAL ~ 10 ppb (Hartley band of ozone)
Resonance Raman ~ ppm
100 ppm – 10 ppb - - - - 100 ppt (?)
Fluorescence ~ 10's of ppm
1 ppm – 10 ppt (?)

ACKNOWLEDGEMENTS

The PSU lidar development, testing, and field investigations have been supported by the following organizations: US Navy through SPAWAR PMW-185, NAVOCEANO, NAWC Point Mugu, ONR, DOE, EPA, Pennsylvania DEP, California ARB, NASA and NSF. The hardware and software development has been possible because of the excellent efforts of several engineers, technicians, and graduate students at PSU in the Applied Research Laboratory and the Department of Electrical Engineering. Special appreciation goes to D. Sipler, B. Dix, Gil Davidson, D.B. Lysak, T.M. Petach, F. Balsiger, T.D. Stevens, P.A.T. Haris, M. O'Brien, S.T. Esposito, K. Mulik, A. Achey, E. Novitsky, G. Li, Sachin Verghese, David Brown, Adam Willitsford, and many graduate students who have made contributions to these efforts. The NE-OPS research investigations have been supported by the USEPA STAR Grants Program #R826373, Investigations of Factors Determining the Occurrence of Ozone and Fine Particles in Northeastern USA, and by the Pennsylvania DEP. The cooperation and collaborations with many university and government laboratory researchers are gratefully acknowledged, in particular the contributions of Rich Clark, S.T. Rao, George Allen, Bill Ryan, Bruce Doddridge, Hans Hallen, Zhiwen Liu, Steve McDow, Delbert Eatough, Susan Weirman, and Fred Hauptman are particularly acknowledged. Major collaborative efforts with Steve Stearns of ITT and with Charlie Ritchey of Michigan Aerospace Corporation are acknowledged.

REFERENCES

[1] Berk, A., et al., "MODTRAN5: A reformulated atmospheric band model with auxiliary species and practical multiple scattering options," in Algorithms and Technologies for Multispectral, Hyperspectral, and Ultraspectral Imagery X, *Proceedings of SPIE*, v. 425, S. Shen, ed., pp. 341 – 347, 2004.

[2] Inaba, H. and T. Kobayasi, "Laser-Raman Radar," Opto-electronics, **4** 101- 123, 1972.

[3] Inaba, H., "Detection of Atoms and Molecules by Raman Scattering and Resonance Fluorescence," in Laser Monitoring of the Atmosphere, (Ed. E.D. Hinkley), Springer-Verlag, 153-236, 1976.

[4] Kobayshi, Takao, "Techniques for Laser Remote Sensing Environment," Remote Sensing Reviews, Vol. 3, pp. 1-56, 1987.

[5] Philbrick, C.R., D.B. Lysak, T.D. Stevens, P.A.T. Haris and Y.-C. Rau,"Atmospheric Measurements Using the LAMP Lidar during the LADIMAS Campaign," 16th International Laser Radar Conference, NASA Pub. 3158, 651-654, 1992.

[6] Rajan, S., T. J. Kane and C. R. Philbrick, "Multiple-wavelength Raman Lidar Measurements of Atmospheric Water Vapor," Geophys. Res. Let. 21, 2499-2502, 1994.

[7] Philbrick, C.R., and K Mulik, "Application of Raman Lidar to Air Quality Measurements," Proceedings of the SPIE Conference on Laser Radar Technology and Applications V, 4035, 22-33, 2001.

[8] Mulik,K.R., and C.R. Philbrick, "Raman Lidar Measurements of Ozone During Pollution Events," in Advances in Laser Remote Sensing, Selected papers from 20th ILRC, Vichy France, pp 443-446, 2001.

[9] Doddridge, Bruce G., Richard D. Clark and C. Russell Philbrick, "Airborne Measurements of Chemistry and Aerosol Optical Properties during NARSTO Northeast Oxidant and Particle Study," Proceedings of the Am. Met. Soc. 4th Conf. Atmo. Chem., 146-152, 2002.

[10] Philbrick, C. Russell, "Overview of Raman Lidar Techniques for Air Pollution Measurements," in Lidar Remote Sensing for Industry and Environment Monitoring II, SPIE , 136-150, 2002.

[11] Philbrick, C. Russell, "Overview of Raman Lidar Techniques for Air Pollution Measurements," in Lidar Remote Sensing for Industry and Environment Monitoring II, SPIE , 136-150, 2002.

[12] Philbrick, C.R., "Raman Lidar Descriptions of Lower Atmosphere Processes," Lidar Remote Sensing in Atmospheric and Earth Sciences, Proc. 21st ILRC, Valcartier, Quebec Canada, 535-545, 2002.

[13] Philbrick, C.R., "Raman Lidar Characterization of the Meteorological, Electromagnetic and Electro-optical Environment," Proc. SPIE Vol. 5887, Lidar Remote Sensing for Environmental Monitoring VI; Upendra N. Singh; Ed., p. 85-99, Aug 2005.

[14] Collier, Paul Jason, "RF Refraction on Atmospheric Paths from Raman Lidar," MS Thesis Penn State University, Department of Electrical Engineering, August 2004.

[15] Willitsford, Adam, C. R. Philbrick, "Lidar Description of the Evaporative Duct in Ocean Environments," Proc. SPIE Vol. 5885, Remote Sensing of the Coastal Oceanic Environment; Robert J. Frouin, Marcel Babin, Shubha Sathyendranath; Eds., p. 140-147, Aug 2005.

[16] Stearns, Steven V., Raymond T. Lines, Christian J. Grund and C. Russell Philbrick, Active Remote Detection of Natural Gas Pipeline Leaks, Technology Status Reports of NETL Department of Energy, web: http://www.netl.doe.gov/scngo/Natural%20Gas/index.html + Projects + Remote Sensing Technologies + Leak Detection + DE-FC26-03NT41877 + Status Assessment

[17] Philbrick, C. Russell, Zhiwen Liu, Hans Hallen, David M. Brown, and Adam Willitsford, "LIDAR Techniques Applied to Remote Detection of Chemical Species in the Atmosphere," C. Russell Proc ISSSR, 2006 http://www.isssr2006.com/TALK_UPLOADS/Russell-Philbrick.pdf

[18] Stearns, Steven V., R. Todd Lines, Darryl G. Murdock, Matthew C. Severski, Dawn D. Lenz, David M. Brown, C. Russell Philbrick, "Airborne Natural Gas Emission Lidar (ANGEL)," System Proc ISSSR, 2006 http://www.isssr2006.com/TALK_UPLOADS/Steven-Stearns.pdf

[19] Alfano, R.R., *Supercontinuum Laser Source,* Springer Verlag, NY 1989.

[20] Begnoché, J. "Analytical Techniques for Laser Remote Sensing with a Supercontinuum White Light Laser" The Pennsylvania State University, M.S. Thesis, 2005.

[21] Brown, David M., Perry S. Edwards, Kebin Shi, Zhiwen Liu, and C. Russell Philbrick, "Supercontinuum LIDAR Measurements of Atmospheric Constituents," Ibid. 2007.